Chlorine activation indoors and outdoors via surface-mediated reactions of nitrogen oxides with hydrogen chloride

Jonathan D. Raff^a, Bosiljka Njegic^a, Wayne L. Chang^b, Mark S. Gordon^c, Donald Dabdub^b, R. Benny Gerber^{a,d}, and Barbara J. Finlayson-Pitts^{a,1}

^aDepartment of Chemistry, University of California, Irvine, CA 92697-2025; ^bDepartment of Mechanical and Aerospace Engineering, University of California, Irvine, CA 92607-3975; ^cDepartment of Chemistry, Iowa State University, Ames, IA 50011; and ^dFritz Haber Research Center for Molecular Dynamics, The Hebrew University, Jerusalem, 91904, Israel

This Feature Article is part of a series identified by the Editorial Board as reporting findings of exceptional significance.

Edited by Jack Halpern, University of Chicago, Chicago, IL, and approved June 4, 2009 (received for review April 15, 2009)

Gaseous HCl generated from a variety of sources is ubiquitous in both outdoor and indoor air. Oxides of nitrogen (NO_y) are also globally distributed, because NO formed in combustion processes is oxidized to NO2, HNO3, N2O5 and a variety of other nitrogen oxides during transport. Deposition of HCl and NO_v onto surfaces is commonly regarded as providing permanent removal mechanisms. However, we show here a new surface-mediated coupling of nitrogen oxide and halogen activation cycles in which uptake of gaseous NO2 or N2O5 on solid substrates generates adsorbed intermediates that react with HCl to generate gaseous nitrosyl chloride (CINO) and nitryl chloride (CINO₂), respectively. These are potentially harmful gases that photolyze to form highly reactive chlorine atoms. The reactions are shown both experimentally and theoretically to be enhanced by water, a surprising result given the availability of competing hydrolysis reaction pathways. Airshed modeling incorporating HCl generated from sea salt shows that in coastal urban regions, this heterogeneous chemistry increases surface-level ozone, a criteria air pollutant, greenhouse gas and source of atmospheric oxidants. In addition, it may contribute to recently measured high levels of CINO2 in the polluted coastal marine boundary layer. This work also suggests the potential for chlorine atom chemistry to occur indoors where significant concentrations of oxides of nitrogen and HCl coexist.

heterogeneous chemistry | lower atmosphere

aseous HCl levels reaching concentrations of a few parts-perbillion (ppb) (vol:vol) have been measured in polluted air and in some indoor settings (1–6). Direct emissions include garbage burning (7), incineration of municipal and medical wastes, burning of biomass, agricultural products and coal, and industrial processes, e.g., semiconductor and petroleum manufacturing (5). Natural sources in air include volcanic eruptions and reactions of sea salt and organochlorine compounds (5). Removal indoors and in the boundary layer is largely by deposition. Because many of these HCl sources involve combustion or occur in polluted urban areas, oxides of nitrogen are typically present simultaneously.

Although heterogeneous nitrogen oxide reactions on airborne particles and boundary layer surfaces are known to be important in the atmosphere, their kinetics and mechanisms remain elusive (8). For example, the hydrolysis of NO₂ on surfaces,

$$2NO_2 + H_2O \xrightarrow{surface} HONO + HNO_3$$
 [1]

generates gas phase nitrous acid (HONO), a major OH source in continental regions (8, 9), and HNO₃. Nitric acid and other, as yet unidentified, oxides of nitrogen, NO_y ($NO_y = NO + NO_2 + HNO_3 + N_2O_5 + ...$), are strongly adsorbed on surfaces and when they are irradiated, generate HONO, NO and NO_2 (10–13), even in sup-

posedly "clean" systems (14). Based on a variety of experimental studies, the surface complex $\mathrm{NO^+NO_3^-}$ has been proposed to be a key intermediate (8) in the hydrolysis of $\mathrm{NO_2}$ and the precursor of HONO in this system:

$$2NO_2 \xrightarrow{\text{surface}} NO^+NO_3^-$$
 [2]

$$NO^+NO_3^- + H_2O \rightarrow HONO + HNO_3.$$
 [3]

Formation of $NO^+NO_3^-$ is thought to be from autoionization of asymmetric N_2O_4 (ONONO₂), possibly formed by sequential uptake and reaction of NO_2 on the surface (15). Recent theoretical studies (16) show that once ONONO₂ is formed, it is converted within femtoseconds to $NO^+NO_3^-$; based on experimental studies of NO_2 on ice films, conversion of $NO^+NO_3^-$ to HONO via reaction [3] is also fast (17, 18). To the best of our knowledge, there are no reports of other reactions of the ion pair that compete with the reaction with water.

In the case of N_2O_5 , autoionization to $NO_2^+NO_3^-$ has also been proposed as a key intermediate step (19, 20), and rapid reaction with water also occurs, forming nitric acid:

$$NO_2^+NO_3^- + H_2O \rightarrow 2HNO_3.$$
 [4]

This article presents a combination of experiments and theory that demonstrate new chemistry in which surface-bound oxides of nitrogen from the uptake of NO₂ or N₂O₅ react with gaseous HCl to form ClNO and ClNO₂, respectively, potentially harmful gases (21) that photolyze to form chlorine atoms. We show that uptake of oxides of nitrogen and HCl on surfaces is not necessarily a permanent removal mechanism, but rather can be an intermediate step on the way to generating more reactive gases. Fundamental molecular insights gained from theoretical calculations confirm the experimental observations that water has a remarkable effect on this chemistry and imply that this chemistry is likely under atmospheric conditions, both outdoors and indoors. Indeed, our airshed model calculations demonstrate the potential importance of this

Author contributions: J.D.R., B.N., W.L.C., M.S.G., D.D., R.B.G., and B.J.F.-P. designed research; J.D.R., B.N., and W.L.C. performed research; J.D.R., B.N., W.L.C., M.S.G., D.D., R.B.G., and B.J.F.-P. analyzed data; and J.D.R., B.N., W.L.C., M.S.G., D.D., R.B.G., and B.J.F.-P. wrote the paper.

The authors declare no conflict of interest.

This article is a PNAS Direct Submission.

Freely available online through the PNAS open access option.

See Commentary on page 13639.

¹To whom correspondence should be addressed. E-mail: bjfinlay@uci.edu.

This article contains supporting information online at www.pnas.org/cgi/content/full/0904195106/DCSupplemental.

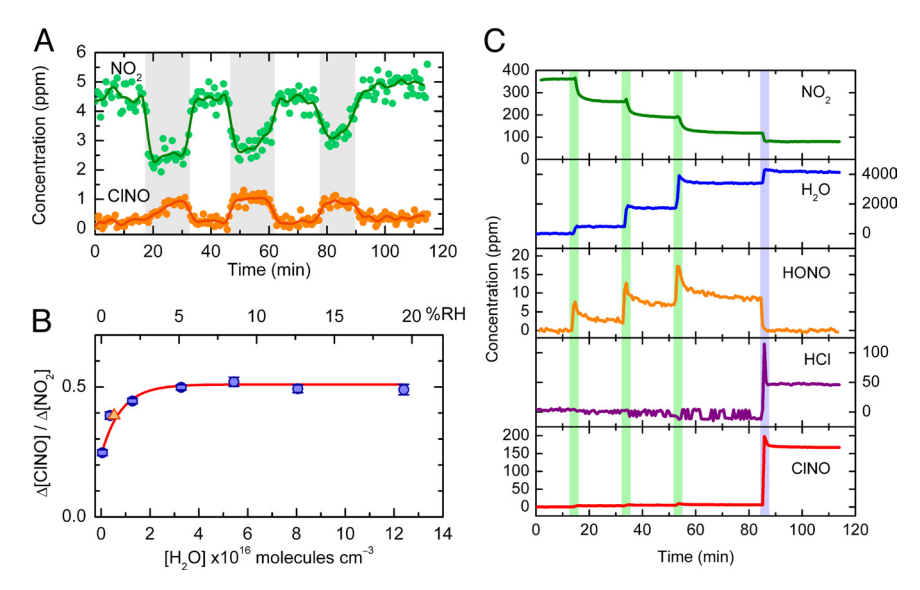


Fig. 1. Reaction of HCl with NO₂ on SiO₂ studied by infrared spectroscopy. (A) Nitrosyl chloride (CINO) is formed efficiently when a stream of gas containing 3.7–5.5 ppm (vol:vol) NO₂, 5–10 ppm (vol:vol) HCl and H₂O (≈0.5% relative humidity) flows over a bed of high-surface area (330 m²) SiO₂ (shaded regions); the reaction does not occur when the stream is diverted through an empty reaction cell (clear regions). (B) The concentration of CINO formed per NO2 reacted increases from 25% in the absence of added water vapor to 50% at a relative humidity (RH) ≥5%; the triangle marks the average CINO yield derived from the experiment described in panel A. The maximum yield expected based on reaction [5] is 0.5. (C) The addition of water vapor has a dramatic effect on gaseous NO₂ initially present in a reaction cell containing SiO_2 pellets. Sequential addition of water vapor (1.6, 3.1, and 3.2 Torr, indicated by green regions) leads to enhanced uptake of NO2 on the SiO2 surfaces and formation of nitrous acid (HONO). Introducing HCI to the chamber (blue region) leads to rapid CINO formation with a yield of 47%, relative to the amount of NO2 initially present. Units of concentration are parts per million by volume (ppmv).

novel chemistry in polluted marine regions where HCl from sea salt reactions and NO_v from urban emissions coexist. It is clear from this work that uptake of oxides of nitrogen and HCl on surfaces may contribute to chemistry and photochemistry in previously unrecognized ways both indoors and outdoors, including in coastal regions and downwind of waste, coal and biomass combustion, and industrial processes that generate HCl.

Results and Discussion

NO₂ Surface Reaction. The experiments use a flow system designed to deliver controlled amounts of NO₂, HCl and water vapor in a stream of nitrogen to one of a set of parallel borosilicate glass reaction chambers before passing through an optical cell in a Fourier transform infrared (FTIR) spectrometer. One chamber contains silica (SiO₂) powder pressed into pellets, which provide large surface areas for the heterogeneous chemistry, whereas the second, empty chamber acts as a bypass. Silica powder is selected to mimic silicate-rich urban surfaces and some of the oxide surfaces present in mineral dust (8, 22, 23), which are important substrates for heterogeneous tropospheric chemistry. Fig. 1A shows that CINO is formed efficiently when a stream of reactants passes through the chamber containing SiO₂, but not the bypass. The likely mechanism involves reaction of NO⁺NO₃ with HCl:

$$NO_2^+NO_3^- + HCl \rightarrow CINO + HNO_3.$$
 [5]

The average ratio of ClNO formed to NO_2 reacted, Δ [ClNO]/ $\Delta[NO_2]$, is 0.39 \pm 0.01 (2 s) at a relative humidity of 0.5%. The reactor containing SiO₂ has $\approx 10^4$ times more surface area than the bypass, and its effect on ClNO formation confirms the heterogeneous nature of the reaction, which is extremely slow in the gas phase (24).

To study the relative humidity dependence, a cell used in static mode (i.e., where reactants are added to the cell and allowed to react in situ) is positioned in the FTIR such that the IR beam interrogates the gas over the top of a bed of SiO₂ pellets. Nitrogen dioxide is introduced from a bulb on the attached vacuum line and anhydrous HCl or a mixture of HCl and water vapor is then added. As shown in Fig. 1B, $\Delta [CINO]/\Delta [NO_2]$ is 0.25 under anhydrous conditions, but doubles to the theoretical yield implied by reactions [2] and [5] when the relative humidity is >5% (3 \times 10¹⁶ molecules cm⁻³). Not only does the conversion of NO₂ to ClNO occur at relative humidities (RH) found in the atmosphere, but surprisingly, water actually enhances the reaction despite the possibility of competition from reaction [3]. A catalytic role of water in thermal and photochemical reactions has been reported for other systems (25–27). However, to the best of our knowledge it has not been reported for a case involving thin water films on a solid substrate where water can also participate in a competing reaction. It is also notable that separate experiments (see SI Text) show that water vapor does not enhance the heterogeneous hydrolysis of ClNO in this system. This suggests that under some conditions, loss of ClNO to aerosol particles and surfaces at the terrestrial-air interface may be much slower than what is expected to occur in bulk water (28, 29).

Fig. 1C shows the effect of adding water alone to a reaction chamber containing NO₂ and SiO₂ pellets. The gas-phase concentration of NO₂ decreases with each addition of water vapor as it is taken upon the SiO₂ surface, facilitating NO₂ uptake, and forming gas phase HONO via reaction [3]. When HCl is added, ClNO is formed rapidly, indicating that under these conditions reaction [5] competes with reaction [3]. Although these experiments are performed using higher mixing ratios than found in the atmosphere, the fact that similar CINO yields are obtained with NO2 concentrations varying over 2 orders of magnitude (Fig. 1 A-C) is a good indication that this chemistry will occur at lower concentrations typically found in air both indoors and outdoors.

Because HONO is known to react with HCl heterogeneously to form ClNO (30, 31), the possibility that HONO is initially formed in reaction [3] and then reacts further with HCl to form ClNO must be considered. This can be ruled out because the amount of CINO that is possible from the direct reaction of HCl with gaseous HONO at 80 min (Fig. 1C) is <3% of the reacted NO₂, much less than observed. This shows that the ClNO precursor must be adsorbed to the SiO₂ surface before the introduction of HCl. Theoretical studies

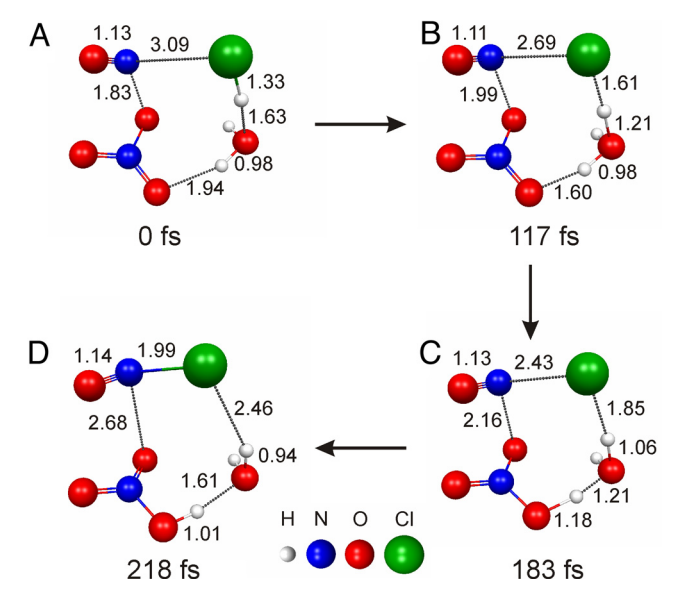


Fig. 2. Snapshots along an ab initio molecular dynamics "on-the-fly" trajectory of CINO formation show how the reaction of HCl and ONONO2 is catalyzed by 1 water molecule. (A) Weakly bound reactive complex formed upon geometry optimization of ONONO2, HCl and H2O. (B) First proton transfer from HCl to H2O to form Cl¹ and H3O¹- (C) Second proton transfer from H3O¹- to NO $_3$ ¯ to form H2O and HNO3. (D) Product CINO is formed. Calculations are carried out at the MP2/cc-pVDZ level of theory. Depicted atomic distances are given in Ångströms. The amount of time elapsed along the trajectory is provided below each structure.

predict that HONO adsorbs to SiO₂ surfaces (32), so that the gaseous HONO observed in Fig. 1*C* could be in equilibrium with far greater amounts of surface-adsorbed HONO or nitrite (although given that HNO₃ is formed simultaneously, HONO will be the major species). However, control experiments in which SiO₂ is exposed to gaseous HONO followed by HCl do not produce ClNO (see *SI Text* and Fig. S1), ruling this pathway out as a major source.

The proposed mechanism and the effect of water in enhancing CINO formation are supported by theory. A series of high level ab initio calculations [using the General Atomic and Molecular Electronic Structure System (GAMESS) (33)] are performed to gain insight into the role of water in CINO formation. The starting reactive species in the calculations is the asymmetric dimer, ON-ONO₂ in gas-phase clusters comprised of HCl and a varying number of water molecules. Previous studies have shown that gas-phase clusters are suitable models for surface reactions where the substrate is not involved in the chemical mechanism (34). Molecular dynamics "on-the-fly" calculations [using second-order perturbation theory (MP2) with the cc-pVDZ basis set, denoted MP2/cc-pVDZ], are performed to elucidate the mechanism (Fig. 2). Water acts as a conduit to transfer a proton from HCl to NO_3^- , facilitating the formation of the products CINO and HNO₃. Energetics are attained at the coupled cluster [CCSD(T)/cc-pVTZ] level of theory by conducting single point energy calculations on the stationary structures obtained on the MP2/cc-pVDZ surface. In the absence of water, the activation energy for CINO formation is 11.5 kcal·mol^{−1}. Addition of 1 water molecule lowers the activation energy to 5.3 kcal·mol⁻¹. The formation of ClNO is exothermic by 10.0 kcal·mol⁻¹ in the absence of water and 12.9 kcal·mol⁻¹ in the presence of 1 water molecule. A barrierless channel is found for CINO formation in the presence of 2 water molecules at the MP2/cc-pVDZ level of theory. Thus, the theoretical results support the experiments described above and demonstrate the critical role of water in enhancing the formation of CINO.

 N_2O_5 Reaction. Gaseous HCl may also react with other oxides of nitrogen such as N_2O_5 on surfaces to form ClNO₂ (35). The

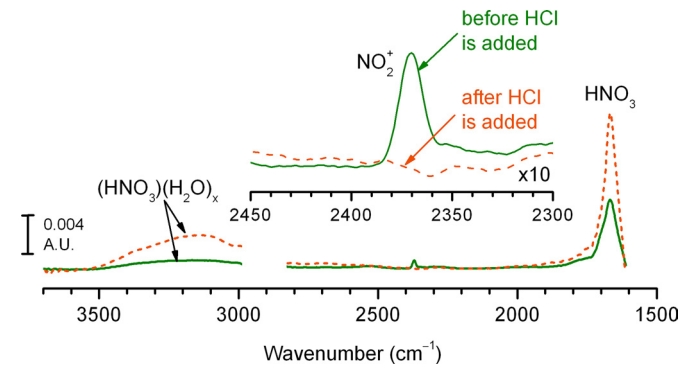


Fig. 3. Nitronium nitrate $(NO_2^+NO_3^-)$ is the key intermediate in reaction of N_2O_5 with HCl on surfaces. ATR-FTIR was used to obtain the spectra of species adsorbed to a ZnSe crystal exposed to 10 Torr of N_2O_5 (solid line) and subsequently 20 Torr of HCl (dashed line) in the absence of added water vapor. (*Inset*) An expanded spectral region where the NO_2^+ infrared absorption band occurs

reaction likely occurs through an analogous mechanism to that for NO₂, whereupon absorption to the surface, N₂O₅ autoionizes to NO $_2^+$ NO $_3^-$ and then reacts with HCl,

$$NO_2^+NO_3^- + HCl \rightarrow CINO_2 + HNO_3$$
 [6

in competition with water, reaction [4]. The gas-phase reaction is otherwise slow in the absence of sufficient surface area (24). Spectral evidence for the role of NO₂⁺ as the key intermediate in reaction of HCl with N2O5 was obtained using attenuated total reflection FTIR (ATR-FTIR) spectroscopy. As shown in Fig. 3, sharp bands at 2,370 cm⁻¹ and 1,667 cm⁻¹, and a weak absorbance between 3,500 and 2,500 cm⁻¹ appear in the spectrum measured immediately after the internal reflection element (IRE) is exposed to 10 Torr of N_2O_5 (solid line). The band at 2,370 cm⁻¹ is assigned to the $\nu_3(NO_2$ -antisymmetric) stretching mode of linear NO_2^+ , consistent with previous observations of this ion in the gas phase and at low temperatures in frozen matrices and on metallic substrates (35–39). The band at 1,667 cm⁻¹ is due to the $\nu_2(NO_2$ antisymmetric) stretch of HNO₃. Broad bands between 3,500 and 2,500 cm⁻¹ are assigned to ν (O–H) stretches of nitric acid complexed to surface-adsorbed water (40). The weak signals typically observed for surface-adsorbed species using ATR-FTIR required the use of higher concentrations than found in the atmosphere. However, ionization of N₂O₅ on surfaces is expected to be operational at lower concentrations as well (19, 20).

Similar to the NO₂ case where water promotes the formation of NO+NO₃ from ONONO₂ (16), water is expected to play an essential role in autoionization of N₂O₅. Indeed, calculations at the MP2/cc-pVDZ level of theory show that ionization of N₂O₅ into a NO₂⁺NO₃⁻ ion pair takes place in the presence of 1 or more water molecules (Fig. 4). The largest effect is observed upon addition of the first water molecule, which triggers an increase in the separation of the $NO_2^{\delta+}$ and $NO_3^{\delta-}$ moieties by 0.2 Å compared with free N_2O_5 . Furthermore, the calculated partial charges on these 2 moieties increase dramatically from $\delta(NO_2^{\delta+}) = +0.127$ and $\delta(NO_3^{\delta-}) =$ -0.127 in the free N₂O₅ molecule, to $\delta(NO_2^{\delta+}) = +0.274$ and $\delta(NO_3^{\delta-}) = -0.284$ in the $(N_2O_5)\cdot(H_2O)$ complex. This trend of increasing separation and partial charges on $NO_2^{\delta+}$ and $NO_3^{\delta-}$ moieties continues upon addition of the second and third water molecules. Hence, water enhances the reactivity of N₂O₅ by promoting the formation of the $(NO_2^+) \cdot (NO_3^-)$ ion pair.

The IR absorption band stemming from NO_2^+ is completely removed and nitric acid bands increase when the IRE is exposed to excess HCl in the ATR-FTIR experiment shown in Fig. 3 (dashed line), supporting the mechanism where surface-adsorbed NO_2^+ is the key intermediate in the conversion of N_2O_5 to ClNO₂ (19, 20).

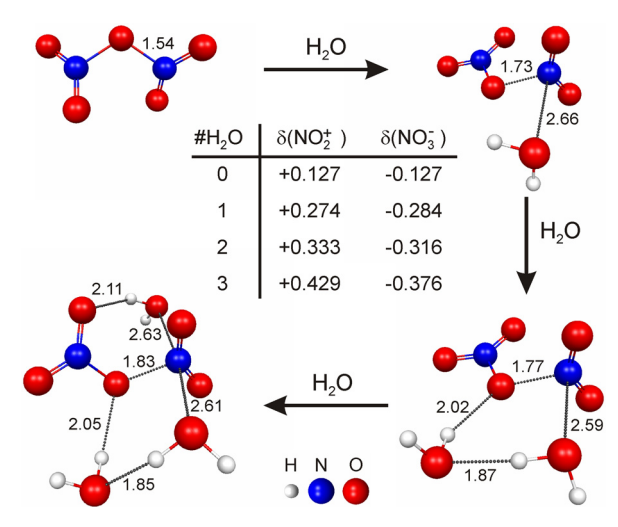


Fig. 4. Geometry optimizations of N₂O₅ in the absence and the presence of 1, 2 and 3 water molecules conducted at MP2/cc-pVDZ level of theory show how ionization and dissociation of N2O5 occurs on water clusters. Depicted atomic distances are given in Ångströms; Mulliken charges on the $NO_2^{\delta+}$ and $NO_3^{\delta-}$ moieties are provided in the table.

In separate experiments (Fig. 5A) using transmission FTIR spectroscopy, ClNO₂ is clearly formed in the gas-phase when HCl is added to a cell containing N2O5. Again, the reaction is more efficient in the presence of water, as demonstrated in Fig. 5B.

Theory again supports the experimental observations and proposed mechanism, showing that water aids the reaction of NO₂⁺ with HCl. The reaction was investigated theoretically by conducting a series of optimizations of the (NO₂⁺)·(HCl) complex in the absence and presence of water at the MP2/cc-pVDZ level of theory. As shown in Fig. 5C, a barrierless channel for the formation of ClNO₂ from NO₂⁺ and HCl is found in the presence of 2 water molecules. Upon addition of the second water molecule the product ClNO₂ is formed having a Cl-N bond length of 2.22 Å and a ∢O–N–O of 144°, comparable to the 1.96 Å and 135° found for the calculated free molecule. Water clearly facilitates the formation of ClNO₂, similar to the trend observed in the ClNO case. There is some similarity to the reactions of ClONO₂ or N₂O₅ with HCl on bulk ice at low temperatures (54); in those cases, Cl⁻ from the dissociation of solvated HCl is the reactive species (35, 41, 42). However, acids at the top of the air-water interface are largely undissociated (34, 40, 43-45). Given this and the fact that water adsorbed on solid substrates at room temperature does not behave like water in the bulk (46–48), it is likely that the reactant in the surface-mediated reaction reported here is molecular HCl.

Atmospheric Implications. Extrapolation to atmospheric conditions both outdoors and indoors relies on similar surface-bound nitrogen oxides being present on real surfaces. Evidence for the universality of reaction [1] is that it has been shown to occur on many different surfaces, including Teflon, borosilicate glass and silica (8), boundary layer surfaces outdoors [e.g., vegetation, building materials etc. (49, 50)], on typical indoor surfaces (51, 52) and on airborne dust particles (50, 53). It is also well known that N₂O₅ is taken up on surfaces and hydrolyzed (54). Due to such uptake, there is a reservoir of strongly adsorbed reactive oxides of nitrogen on surfaces in both environmental chambers (14) and in the field (13).

Experiments were performed at RH up to 25%, typical of drier environments. However, the role of water suggests that this chemistry will continue to higher RH. When gaseous HCl is present as well as oxides of nitrogen, e.g., in coastal areas and downwind of certain industrial settings, incineration facilities (5), biomass burning (55), in buildings such as medieval

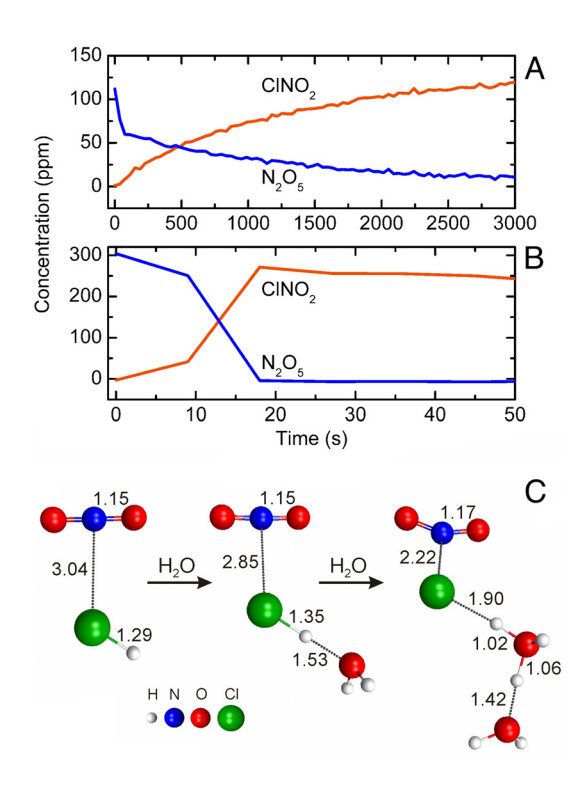


Fig. 5. Reaction of N₂O₅ with HCl in absence and then in the presence of added water vapor. (A) Nitryl chloride (CINO₂) is formed essentially quantitatively (96% yield) as 300 ppm of anhydrous HCl is added at t = 0 to a reaction chamber (volume 64 cm³) containing 126 ppm N₂O₅. Rapid uptake of N₂O₅ onto walls leads to the drop in N₂O₅ levels initially. (B) The rate of reaction of N_2O_5 (300 ppm) with HCl vapor (400 ppm) is increased in the presence of water vapor (≈25% relative humidity). Note the different time scales in A and B. Units of concentration are parts per million by volume (ppmv). (C) Ab initio calculations show that the reaction between HCl and NO₂⁺ is catalyzed by water. Minima are obtained by optimizations carried out in the absence and presence of 1 and 2 water molecules at MP2/cc-pVDZ level of theory. The number of water molecules was increased by placing an additional water molecule 4 Å apart from previously obtained structure. Depicted atomic distances are given in Ångströms.

churches and in volcanic plumes (2, 5), it will be converted to ClNO and ClNO₂. ClNO absorbs light well into the visible region (Fig. 6), forming Cl + NO with unit quantum yield (54). As seen in Fig. 6, its absorption cross section in the near UV overlaps strongly not only with solar radiation but also with that from typical fluorescent lights used indoors. Formation of CINO indoors is certainly possible. Indoor surfaces are frequently exposed to NO_y generated from indoor combustion sources or from an influx of polluted outside air (56). It has been proposed that corrosive chlorine containing gases such as HCl [e.g., from cigarette smoke, decomposition of chlorinecontaining polymers, and cleaning agents] are responsible for observed elevated levels of Cl⁻ found in indoor relative to outdoor air (57). Thus, if formed indoors, CINO could serve as a source of highly reactive chlorine atoms that would participate in the complex chemistry known to occur there (52, 58). In addition, the presence of CINO in the indoor environment could have important ramifications for the reliability and lifetime of electronics susceptible to corrosion (59). To the best of our knowledge, chlorine atom chemistry has not been considered in typical indoor air environments.

Outdoors, ClNO and ClNO₂ are important chlorine atom precursors on short time scales because of their rapid photolysis, having calculated lifetimes of only 5 and 30 min, respectively, at a solar zenith angle of 0° (54). Hydrochloric acid also forms Cl atoms

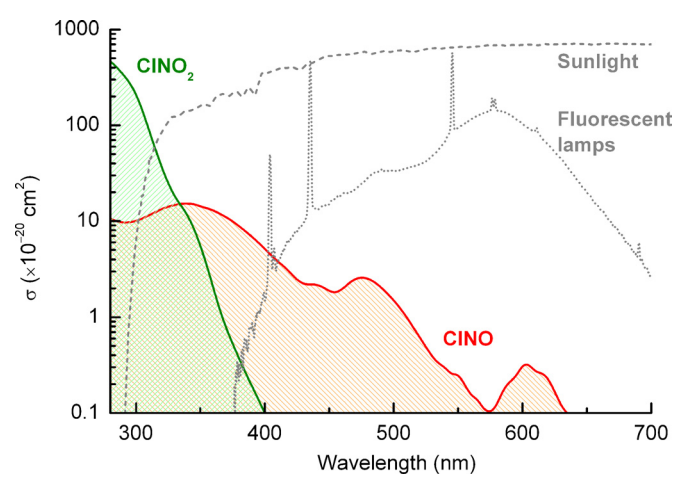


Fig. 6. The overlap between the UV-vis absorption spectra of CINO (104, 105) and $CINO_2$ (104) and emission spectra from the Sun (106) and fluorescent lamps typical of indoor settings.

through its reaction with OH, but this is slow, with a lifetime for HCl with respect to this reaction of $\approx\!14$ days at an OH concentration of 10^6 radicals cm $^{-3}$. In the presence of sufficient NO, chlorine atoms enhance the formation of ozone through well-known organic-NO $_y$ cycles (54) so heterogeneous HCl-to-ClNO conversion could speed up the formation of ozone and other photochemically generated species in polluted coastal urban areas, changing their peak concentration and geographical distribution. Ozone is an important trace gas with documented health effects, a greenhouse gas, and a significant atmospheric oxidant and precursor to the OH radical (54).

The potential role of heterogeneous HCl-to-ClNO conversion in a coastal airshed (see Fig. S2) is probed using a model (60) that employs state-of-the-art modules for both gas-phase and heterogeneous/multiphase reaction mechanisms, and dynamic aerosol predictions (60, 61). Although this model represents the Southern California air basin, it is typical of polluted coastal regions elsewhere. Two simulations are examined: A base case that provides benchmark predictions of the ambient concentrations of O₃, ClNO and HCl without the surface mediated conversion, and a test case that assumes that every HCl molecule deposited generates 1 gaseous CINO molecule. This in effect assumes that HCl is the limiting reagent. Although this might appear to be the extreme case, it is not necessarily the upper limit for conversion of HCl to ClNO because the reaction probability in the model is expressed as a function not only of the deposition velocity of HCl but also of the total surface area of the domain. Surface areas in the model do not include the additional geometric area due to structures such as buildings, nor the molecular scale porosity of surfaces; these can contribute significantly to chemistry in the boundary layer (50). It also assumes that HCl will continue to compete with water vapor for the NO+NO₃ intermediate under typical atmospheric conditions. The ratio of HCl/H₂O that was experimentally accessible here was typically of the order of 10^{-3} whereas in air, it is $\approx 10^{-6}$ to 10^{-7} . Whether this assumption is justified awaits measurement of the relative rate constants for reactions [3] and [5].

Fig. 7A shows the geographical distribution and concentrations of O_3 , ClNO and HCl at the times at which they each peak within the modeling domain. Fig. 7B shows the increase in concentrations, ΔO_3 , $\Delta ClNO$, and ΔHCl , above those predicted for the base case due to the inclusion of surface-mediated HCl-to-ClNO conversion. The locations with the greatest impact from the new ClNO source are mainly in the downwind regions of the domain and show up to 40 ppb more O_3 ($\approx 20\%$ increase) in a 1-h averaging time relative to the base case, and up to 25 ppb increase over an 8-h averaging

time. For comparison, the current U.S. Environmental Protection Agency (EPA) 8-h average standard is 75 ppb. Additional test cases performed with varying conversion probabilities suggest that increases in ozone levels scale linearly with the HCl-to-ClNO conversion probability so that a smaller ClNO yield generates proportionally smaller amounts of O₃ above the base case.

It is noteworthy that this heterogeneous chemistry of oxides of nitrogen with gaseous HCl is the inverse of mechanisms of chlorine activation from sea salt particles in coastal areas involving chloride, which can generate a variety of photochemically active chlorine atom precursors (5, 62–64). For example, reactions of gaseous NO₂ and N2O5 with chloride ions in sea salt particles are known to generate ClNO and ClNO₂ (20, 63-66). Although the former reaction is likely too slow to generate significant amounts of CINO in coastal environments, the latter is believed to be responsible for the formation of ClNO₂ measured recently in air (67), where measured mixing ratios of $CINO_2$ were greater than expected based on the measured concentrations of N₂O₅ and chloride in sea salt particles. It is possible that the chemistry reported here may have contributed to the measured ClNO₂. This heterogeneous chemistry is also expected to be important around salt lakes such as the Dead Sea (68) and the Great Salt Lake (69), and during dust storms where enhanced HCl uptake has been observed (70). Plumes from biomass (55) and garbage burning (7) are other cases where this chemistry may be significant in outdoor environments.

Unusual chlorine activation near the midlatitude tropopause has been reported that appears to be associated with high particle surface areas, relatively high water vapor concentrations and mixing of tropospheric and stratospheric air (71). Although reaction of HCl with ClONO₂ on polar stratospheric clouds (PSCs) in polar regions is known to generate Cl₂, this unusual midlatitude chemistry does not appear to require PSCs. The heterogeneous reaction of HCl with surface-bound oxides of nitrogen to form ClNO would be consistent with the need for high surface areas and water vapor for midlatitude tropopause chlorine activation.

In short, the combination of experiments and theory reported here suggests a new and unique coupling of surface-mediated nitrogen oxide and halogen activation cycles that will generate CINO and CINO₂ in a wide variety of outdoor air environments, and indoors where it has not been considered. Although a technique to measure CINO₂ at ppt levels has been developed (67), this is not the case for CINO, but is clearly needed. Similar chemistry is expected for HBr, leading to photolyzable bromine species such as BrNO and BrNO₂ that cause O₃ destruction through well-known cycles (54).

Materials and Methods

Experimental Details. Infrared spectra were collected using a Thermo Nicolet Avatar 370 Fourier transform infrared (FTIR) spectrometer equipped with a liquid nitrogen-cooled Hg-Cd-Te (MCT) detector. Background single beam spectra were obtained from the average of 200–2,000 interferograms whereas single beam spectra collected during the reaction were obtained from the average of 6–2,000 interferograms; in all cases, spectra were recorded at 1-cm⁻¹ resolution. The IR transmission cells were made of borosilicate glass with an optical path length of either 12 or 10 cm and an inner diameter of 2.5 cm. The ends were closed with germanium windows and sealed with Viton "O"-rings. Concentrations of NO₂, CINO and H₂O were determined from calibrations measured in our laboratory. Absolute cross sections of nitrous acid from Barney et al. (72) were applied. Hydrogen chloride absorption cross sections were obtained from a reference spectrum available in the Pacific Northwest National Laboratory vapor phase infrared spectral library (73). All experiments were conducted at 22 ± 1 °C under dark conditions.

Gases were handled with an all-glass vacuum line with Teflon stopcocks and Kalrez "O"-rings. Nitrogen dioxide was synthesized from the reaction of NO (Matheson, 99%) with excess oxygen (Oxygen Service, 99.993%), followed by trap-to-trap purification. Nitric oxide was purified by passing it through an acetone/dry ice bath trap at 195 K before use. Nitrosyl chloride (CINO) was synthesized from the reaction of 1 eq of Cl₂ (Matheson, 99.5%) and slightly more than 2 eq of nitric oxide, followed by repeated freeze-thaw cycles at liquid nitrogen temperatures to drive the reaction to completion in the liquid phase.

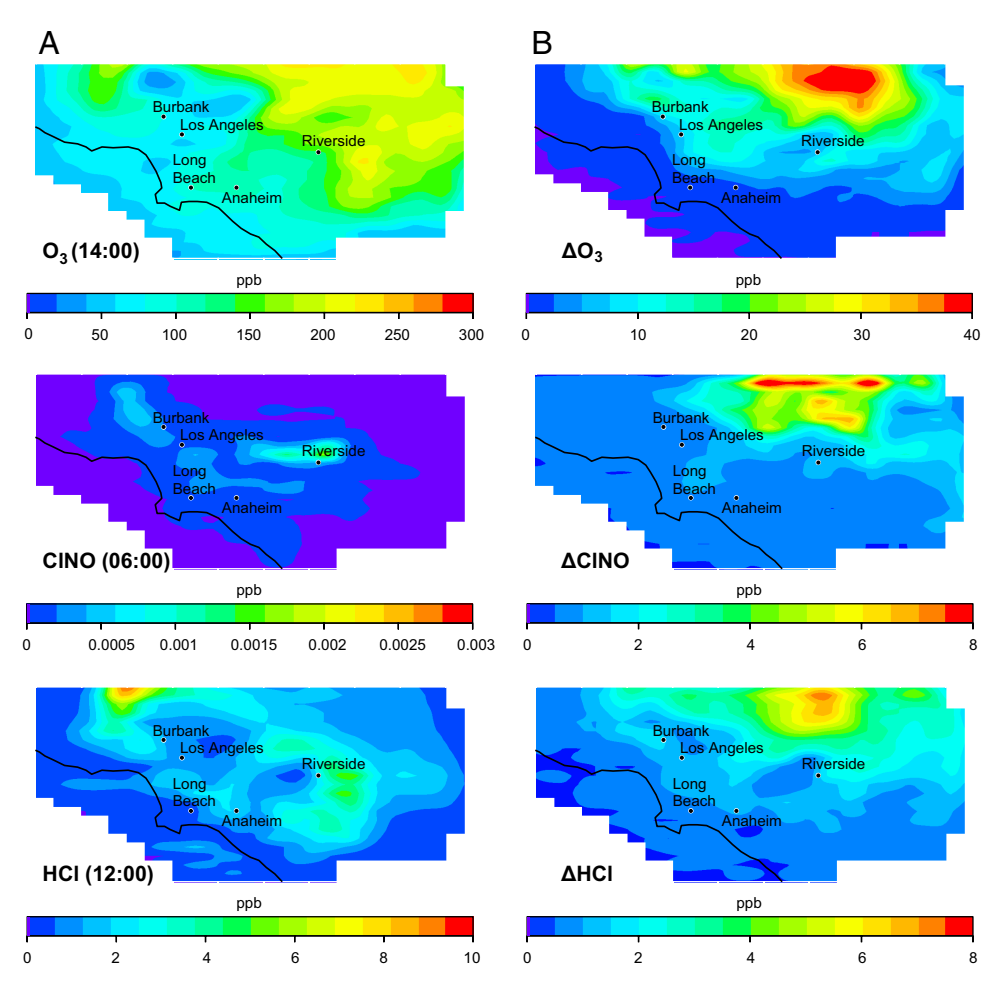


Fig. 7. Impact of HCI-NO2 chemistry on ambient air quality in the South Coast Air Basin (SoCAB) of California. Shown are the domain-wide time maxima mixing ratios in parts-per-billion by volume (ppbv) for the base case (A). The peaks occur at 14:00, 6:00, and 12:00 for O₃, CINO, and HCI, respectively. The increases over the values in A for O₃, CINO, and HCl at the same hours for O₃, CINO, and HCl are shown in B, i.e., these are the additional concentrations on top of those predicted for the base case due to inclusion of the heterogeneous HCl-to-CINO conversion.

The vessel containing CINO was held at 195 K and the excess nitric oxide and chlorine were removed under vacuum until a constant vapor pressure above the CINO was attained. Nitrosyl chloride purified this way was determined to be ≥99.9% pure by FTIR (42.5 m path length). Dinitrogen pentoxide (N₂O₅) was synthesized by reacting 2 eq of NO₂ with slightly more than 1 eq of ozone (from a 3% mixture in O₂) in a previously conditioned glass bulb equipped with a cold finger. The cold finger was cooled to 195 K to condense N₂O₅; oxygen and unreacted ozone were removed under vacuum. The N_2O_5 was stored at 195 K in a storage tube under vacuum and in the dark. The product was ${\approx}95\%$ pure (determined by FTIR, 10 cm path length) with the main impurities being HNO₃ and NO2. Nitrous acid was generated by the method of Wingen et al. (31). Silica pellets were formed by hand pressing SiO₂ powder (Cab-O-Sil, Cabot) in a precleaned stainless steel press. The SiO₂ powder was baked overnight at 475 °C before pressing to remove adsorbed organic impurities and a new batch of pellets were used for each experiment.

Studies of the NO₂ + HCl reaction. The flow system used to study the reaction of HCl with surface-adsorbed NO₂ was constructed of Teflon PFA and designed to deliver a controlled amount of NO₂ (5% in Ultrapure grade N₂, Scott-Marrin) and HCl (from the vapor over a 5 M aqueous solution at 22 °C) in a stream of nitrogen to 1 of 2 parallel borosilicate glass reaction chambers (each with $V=64~{\rm cm}^3$) before finally passing through the IR cell (12 cm path length) at a flow rate of 75 cm³·min⁻¹. One chamber was filled with 1.0 g of fumed SiO₂ (Cab-O-Sil from Cabot) which had been pressed into pellets and broken into pieces that were ≈5 mm in each dimension. The total fumed SiO₂ surface area was measured previously using the Brunauer-Emmett-Teller (BET) method and found to be 329 m²·g⁻¹ (74), resulting in a total surface area of 329 m² inside the reactor. The second chamber (geometric surface area of 0.01 m²) was empty and acted as a bypass to allow measurement of the initial concentrations of NO₂, HCl, and H₂O in the reactant mixture. Single beam spectra were continuously collected as the stream of NO₂ (5 ppm), HCl (10 ppm) and water vapor (≈0.5% relative humidity measured using the infrared absorbance of selected water lines) was alternated between flowing through the empty or SiO₂-filled chamber. Uptake of NO₂ on the SiO₂ surface decreases somewhat over time, likely due to the dehydration of the surface with repeated exposures. In addition, water may be tied up in complexes of (HNO₃)·(H₂O)_n as nitric acid (40) accumulates on the surface according to reaction [1].

Measurements of the relative humidity dependence of the CINO yield from the HCl + NO₂ reaction were carried out in a static system using a 10-cm path length IR cell ($V = 43 \text{ cm}^3$) containing 1.0 g of fumed SiO₂ pellets. The IR cell was evacuated overnight at $\approx 10^{-4}$ Torr and heated at 125 °C to drive off most of the surface-adsorbed water before each experiment. After cooling to room temperature, NO_2 was introduced from a bulb on the attached vacuum line. After ≈ 10 min, the IR cell was opened for 10 s to an attached 493-cm³ bulb containing anhydrous HCI (99.995%, Matheson) or a mixture of HCI and water vapor. The concentration range of NO₂ used in these experiments was 35–200 ppm; the amount of HCl added to the IR cell was between 150-800 ppm. These experiments were limited to ≤20% RH because of the strong absorption of water vapor in the infrared, and condensation of water in the mixing bulb used to prepare the HCl/H₂O mixture that would be needed to give higher RH once it was expanded into the reaction cell.

Studies of the N₂O₅ + HCl reaction. Before experiments, the surface inside an empty 10-cm path length IR cell is conditioned by repeated exposure to \approx 1 Torr of N₂O₅ from a preconditioned 4-L glass bulb, followed by evacuation for 1 h at ${\approx}10^{-4}$ Torr to eliminate adsorbed water and reduce the loss rate of N_2O_5 to the walls. For the reaction, N_2O_5 is added to the IR cell. After ≈ 10 min, anhydrous HCl or a mixture of HCl and water vapor is added from a 493-cm³ glass bulb attached

to the IR cell. Addition of HCl occurs at t=0 in Fig. 5 A and B. Spectra of surface-adsorbed NO $_2^+$ before and and after the reaction with HCl (Fig. 3) are obtained with an ATR probe (Axiom Analytical) mounted in the sample compartment of the spectrometer and inserted into a vacuum-tight borosilicate glass reaction chamber (80 cm³). The internal reflection element (IRE) installed at the end of the probe is a ZnSe rod, 0.6 cm dia. \times 4 cm long with 45° conical ends. Interior surfaces of the reaction chamber are first conditioned by repeated exposure to \approx 10 Torr of N $_2$ O $_5$, followed by evacuation for 15 min at \approx 10 $^{-4}$ Torr. The IRE is then exposed to 10 Torr of anhydrous N $_2$ O $_5$ for 30 min before introducing 20 Torr of anhydrous HCl from a bulb on the attached vacuum line.

Computational Details. Ab initio calculations (33, 75) are performed with second-order Møller-Plesset (76–78) (MP2) perturbation theory using the cc-pVDZ basis set (79, 80). Geometry and saddle point optimizations (81–83) are carried out with the largest component of the analytic gradient (76, 84) being smaller than 10^{-5} Hartree/Bohr. Double differencing of analytic gradients is used in the Hessian calculations (85). Minima are confirmed by an all-positive Hessian, whereas transition states have only 1 negative Hessian eigenvalue. Intrinsic reaction coordinate calculations (86–90) are conducted to connect the transition state with the corresponding minima. Molecular dynamics calculations (91–95) "on-the-fly" that have been successfully applied in related studies (34) are performed starting from the located minimum structure that is obtained upon the geometry optimization of ONONO₂, H₂O and HCl.

To attain high accuracy of reported activation energies and reaction enthalpies, single point energy coupled cluster calculations [CCSD(T) (96, 97)] with the cc-pVTZ basis set (79, 80) are performed on the stationary structures already located on the MP2/cc-pVDZ potential energy surface. Zero point energy (ZPE) contributions to the activation energy are calculated by scaling the MP2/cc-pVDZ harmonic ZPE by 0.95 (98). All of the calculations are carried out using the GAMESS (33, 75) package and MacMoIPlot (99) is used for molecular visualization.

Airshed Model Details. The emission inventory selected for the University of California Irvine-California Institute of Technology airshed model simulations of this study is from August 6, 1997, which was used in the 2003 Air Quality Management Plan designed by the South Coast Air Quality Management District of California. A map of the airshed and surrounding areas is shown in Fig. 52. The

- Keene WC (1995) in Naturally-Produced Organohalogens, eds Grimvall A, Leer EWBd (Kluwer Academic, Dordrecht, The Netherlands), pp 363–373.
- Loupa G, Charpantidou E, Karageorgos E, Rapsomanikis S (2007) The chemistry of gaseous acids in medieval churches in Cyprus. Atmos Environ 41:9018–9029.
- 3. Loupa G, Rapsomanikis S (2008) Air pollutant emission rates and concentrations in medieval churches. *J Atmos Chem* 60:169–187.
- 4. Pszenny AAP, et al. (1993) Evidence of inorganic chlorine gases other than hydrogen chloride in marine surface air. *Geophys Res Lett* 20:699–702.
- Keene WC, et al. (1999) Composite global emissions of reactive chlorine from anthropogenic and natural sources: Reactive chlorine emissions inventory. J Geophys Res 104:8429–8440.
- Kim S, et al. (2008) Airborne measurements of HCl from the marine boundary layer to the lower stratosphere over the North Pacific Ocean during INTEX-B. Atmos Chem Phys Discuss 8:3563–3595.
- Christian TJ, et al. (2009) Trace gas and particle emissions from domestic and industrial biofuel use and garbage burning in central Mexico. Atmos Chem Phys Discuss 9:10101–10152.
- Finlayson-Pitts BJ, et al. (2003) The heterogeneous hydrolysis of NO₂ in laboratory systems and in outdoor and indoor atmospheres: An integrated mechanism. *Phys Chem Chem Phys* 5:223–242.
- 9. Stutz J, et al. (2004) Relative humidity dependence of HONO chemistry in urban areas. *J Geophys Res* 109:D03307.
- Kleffmann J (2007) Daytime sources of nitrous acid (HONO) in the atmospheric boundary layer. ChemPhysChem 8:1137–1144.
- 11. Schuttlefield J, et al. (2008) Photochemistry of adsorbed nitrate. J Am Chem Soc 130:12210–12211
- Zhou X, et al. (2003) Nitric acid photolysis on surfaces in low-NOx environments: Significant atmospheric implications. Geophys Res Lett 30:2217.
- Zhou X, et al. (2002) Photochemical production of nitrous acid on glass sample manifold surface. Geophys Res Lett 29:1681.
- Rohrer F, et al. (2005) Characterisation of the photolytic HONO-source in the atmosphere simulation chamber SAPHIR. Atmos Chem Phys 5:2189–2201.
- Pimentel A, S., Lima F, C. A., da Silva A, B. F (2007) The isomerization of dinitrogen tetroxide: O₂N-NO₂ → ONO-NO₂. J Phys Chem A 111:2913–2920.
- Miller Y, Finlayson-Pitts BJ, Gerber RB (2009) Ionization of N₂O₄ in contact with water: Mechanism, timescales and atmospheric implications. J Am Chem Soc, 10.1021/ja900350g.
- Wang J, Koel B (1999) Reactions of N₂O₄ with ice at low temperatures on the Au(111) surface. Surf Sci 436:15–28.
- Wang J, Koel BE (1998) IRAS studies of NO₂, N₂O₃, and N₂O₄ adsorbed on Au(111) surfaces and reactions with coadsorbed H₂O. J Phys Chem A 102:8573–8579.

emission profiles are coupled with meteorological measurements from August 28, 1987 that have been used widely to test air quality models (100, 101). The airshed source function for sea-salt particles is a function of the wind speed (102), and the RH ranged from 30-64%. In this study, the strength of the sea-salt particle source function is that of Cohan et al. (61), which predicts peak HCl concentrations for the base case (Fig. 7A) that are similar to those reported by Keene et al. in New England coastal air [0.005-5.7 ppb (103)] and Osthoff et al. [0.2–1.8 ppb (67)] near the coastline of Houston, TX. The HCI levels for the test case are in some regions a factor of 2 greater than those in the base case due to a positive feedback from CINO formation. Chlorine atoms from CINO photolysis react with volatile organic compounds through H-abstraction reactions to form HCl, which then drives further HCl-to-CINO conversion (54). Chlorine formation initiated by the heterogeneous reaction of the hydroxyl radical with chloride ions at the gas-liquid interface of deliquesced salt particles (60, 62) was not included in the mechanism but would increase the HCl concentration and hence the CINO and O₃. Although additional CINO production pathways may exist, the current approach aims to provide insight into the importance of the proposed HCI-to-CINO conversion chemistry and to understand how ambient ozone levels respond to this source.

Summary. This work shows that when both HCl and oxides of nitrogen coexist indoors or outdoors, their interaction with surfaces does not result solely in their removal by deposition, but rather can also lead to the formation of new photochemically active gases. Particularly surprising is that this chemistry is enhanced by the presence of water, which has important implications not only for the chemistry occurring in the atmosphere but also for the fundamental chemical insights it provides. Clearly, the role of this chemistry needs to be further explored, particularly in indoor air environments where chlorine atoms have not been recognized as potential oxidants.

ACKNOWLEDGMENTS. We thank Eric S. Saltzman and Michael J. Lawler for helpful discussions; Jörg Meyer for constructing custom glassware; and James N. Pitts, Jr. for comments on the manuscript. This work was carried out by AirUCl, an Environmental Molecular Sciences Institute funded by National Science Foundation Grant CHE-0431312. This work was supported by a National Science Foundation Fellowship under National Science Foundation Grant CHE-0836070 (to J.D.R.) and The Air Force Office of Scientific Research (M.S.G.).

- Mozurkewich M, Calvert JG (1988) Reaction probability of nitrogen oxide (N₂O₅) on aqueous aerosols. J Geophys Res 93:15,889- 815:896.
- Behnke W, George C, Scheer V, Zetzsch C (1997) Production and decay of CINO₂ from the reaction of gaseous N₂O₅ with NaCl solution: Bulk and aerosol experiments. J Geophys Res 102:3795–3804.
- 21. Last JA (1991) Global atmospheric change: Potential health effects of acid aerosol and oxidant gas mixtures. *Environ Health Perspect* 96:151–157.
- Lam B, et al. (2005) Chemical composition of surface films on glass windows and implications for atmospheric chemistry. Atmos Environ 39:6578–6586.
- Diamant RME (1970) The Chemistry of Building Materials (Business Books Limited, London).
- Cantrell CA, et al. (1987) Reactions of nitrate radical and nitrogen oxide (N₂O₅) with molecular species of possible atmospheric interest. J Phys Chem 91:6017–6021.
- Donaldson DJ, Vaida V (2006) The influence of organic films at the air-aqueous boundary on atmospheric processes. Chem Rev 106:1445–1461.
- Voehringer-Martinez E, et al. (2007) Water catalysis of a radical-molecule gas-phase reaction. Science 315:497–501.
- 27. Vaida V (2009) Spectroscopy of photoreactive systems: Implications for atmospheric chemistry. *J Phys Chem A* 113:5–18.
- Karlsson RS, Ljungström EB (1996) Laboratory study of CINO: Hydrolysis. Environ Sci Technol 30:2008–2013.
- Scheer V, et al. (1997) Uptake of nitrosyl chloride (NOCI) by aqueous solutions. J Phys Chem A 101:9359–9366.
- Fenter FF, Rossi MJ (1996) Heterogeneous kinetics of HONO on H₂SO₄ solutions and on ice: Activation of HCl. J Phys Chem 100:13765–13775.
- Wingen LM, et al. (2000) A unique method for laboratory quantification of gaseous nitrous acid (HONO) using the reaction HONO + HCl → CINO + H₂O. J Phys Chem A 104:329–335.
- 32. Thompson KC, Margey P (2003) Hydrogen bonded complexes between nitrogen dioxide, nitric acid, nitrous acid and water with SiH₃OH and Si(OH)₄. Phys Chem Chem Phys 5:2970–2975.
- 33. Dykstra CE, Frenking G, Kim KS, Scuseria GE (2005) in *Theory and Applications of Computational Chemistry: The First Forty Years* (Elsevier, Oxford).
- Miller Y, Gerber RB (2008) Dynamics of proton recombination with NO₃⁻ anion in water clusters. Phys Chem Chem Phys 10:1091–1093.
- Sodeau JR, Roddis TB, Gane MP (2000) A study of the heterogeneous reaction between dinitrogen pentoxide and chloride ions on low-temperature thin films. J Phys Chem A 104:1890–1897.
- 36. Bryant G, Jiang Y, Grant E (1992) The vibrational structure of the NO_2 cation. Chem Phy Lett 200:495–501.

- 37 Forney D. Thompson WE, Jacox ME (1993) The vibrational spectra of molecular ions isolated in solid neon. XI. Nitryl ion, nitrite, and nitrate (NO₂⁺, NO₂⁻, and NO₃⁻). J Chem Phys 99:7393-7403
- 38. Koch TG, et al. (1995) A low-temperature reflection-absorption infrared spectroscopic study of ultrathin films of dinitrogen tetroxide and dinitrogen pentoxide on gold foil. J Phys Chem 99:8362-8367.
- 39. Agreiter J, Frankowski M, Bondybey VE (2001) Ionization and hydrolysis of dinitrogen pentoxide in low-temperature solids. Low Temp Phys 27:890-894.
- 40. Ramazan KA, et al. (2006) New experimental and theoretical approach to the heterogeneous hydrolysis of NO₂: The key role of molecular nitric acid and its complexes with water. J Phys Chem A 110:6886-6897.
- 41. Bianco R, Hynes JT (1999) A theoretical study of the reaction of $CIONO_2$ with HCl on ice. J Phys Chem A 103:3797-3801.
- 42. Bianco R, Hynes JT (2006) Heterogeneous reactions important in atmospheric ozone depletion: A theoretical perspective. Acc Chem Res 39:159-165.
- 43. Shamay ES, Buch V, Parrinello M, Richmond GL (2007) At the water's edge: Nitric acid as a weak acid. J Am Chem Soc 129:12910-12911.
- 44. Bianco R, Wang S, Hynes JT (2007) Theoretical study of the dissociation of nitric acid at a model aqueous surface. J Phys Chem A 111:11033-11042.
- 45. Ardura D, Donaldson DJ (2009) Where does acid hydrolysis take place? Phys Chem Chem Phys 11:857-863.
- 46. Moussa SG, et al. (2009) Experimental and theoretical characterization of adsorbed water on self-assembled monolayers: Understanding the interaction of water with atmospherically relevant surfaces. J Phys Chem A 113:2060-2069.
- 47. Thiel PA, Madey TE (1987) The interaction of water with solid-surfaces fundamental-aspects. Surf Sci Rep 7:211-385.
- 48. Maccarini M (2007) Water at solid surfaces: A review of selected theoretical aspects and experiments on the subject. Biointerphases 2:MR1-MR15.
- Stutz J, Alicke B, Neftel A (2002) Nitrous acid formation in the urban atmosphere: Gradient measurements of NO2 and HONO over grass in Milan, Italy. J Geophys Res, 10.1029/2001JD000390.
- 50. Yu Y, et al. (2009) Observations of high rates of NO2-HONO conversion in the nocturnal atmospheric boundary layer. Atmos Chem Phys Discuss 9:183–223.
- 51. Pitts JN, Wallington TJ, Biermann HW, Winer AM (1985) Identification and measurement of nitrous acid in an indoor air environment. Atmos Environ 19:763-767.
- Morrison G (2008) Interfacial chemistry in indoor environments. Environ Sci Tech 42:3494-3499
- 53. Wang S, et al. (2003) Atmospheric observations of enhanced NO₂-HONO conversion on mineral dust particles. Geophys Res Lett 30:1595.
- 54. Finlayson-Pitts BJ, Pitts JN, Jr. (2000) Chemistry of the Upper and Lower Atmosphere—Theory, Experiments, and Applications (Academic, San Diego).
- Yokelson RJ, Christian TJ, Karl TG, Guenther A (2008) The tropical forest and fire emissions experiment: Laboratory fire measurements and synthesis of campaign data. Atmos Chem Phys 8:3509-3527.
- 56. Weschler CJ. Brauer M. Koutrakis P (1992) Indoor ozone and nitrogen dioxide: A potential pathway to the generation of nitrate radicals, dinitrogen pentoxide, and nitric acid indoors. Environ Sci Technol 26:179-184.
- 57. Sinclair JD, Psota-Kelty LA, Weschler CJ (1985) Indoor/outdoor concentrations and indoor surface accumulations of ionic substances. Atmos Environ 19:315-323
- Weschler CJ, Little JC (2007) Chemical and physical factors that influence pollutant dynamics in indoor atmospheric environments. Atmos Environ 41:3109-3110.
- 59. Sinclair JD, Psota-Kelty LA, Weschler CJ, Shields HC (1990) Deposition of airborne sulfate, nitrate, and chloride salts as it relates to corrosion of electronics. J Electrochem Soc 137:1200-1206.
- 60. Knipping EM, Dabdub D (2003) Impact of chlorine emissions from sea-salt aerosol on coastal urban ozone. Environ Sci Technol 37:275-284.
- Cohan A, Chang W, Carreras-Sospedra M, Dabdub D (2008) Influence of sea-salt activated chlorine and surface-mediated renoxification on the weekend effect in the South Coast Air Basin of California. Atmos Environ 42:3115-3129
- 62. Knipping EM, et al. (2000) Experiments and simulations of ion-enhanced interfacial chemistry on aqueous NaCl aerosols. Science 288:301-306.
- $63. \ \ Finlays on \text{-Pitts BJ} \ (2003) \ The \ tropospheric chemistry \ of seasalt: A \ molecular \text{-level view}$ of the chemistry of NaCl and NaBr. Chem Rev 103:4801-4822.
- 64. Rossi MJ (2003) Heterogeneous reactions on salts. Chem Rev 103:4823-4882.
- 65. Finlayson-Pitts BJ (1983) Reaction of NO₂ with NaCl and atmospheric implications of NOCI formation. Nature 306:676-677.
- 66. Livingston FE, Finlayson-Pitts BJ (1991) The reaction of gaseous N_2O_5 with solid NaCl at 298 K: Estimated lower limit to the reaction probability and its potential role in tropospheric and stratospheric chemistry. Geophys Res Lett 18:17-21.
- 67. Osthoff HD, et al. (2008) High levels of nitryl chloride in the polluted subtropical marine boundary layer. Nat Geosci 1:324-328.
- 68. Hebestreit K, et al. (1999) DOAS measurements of tropospheric bromine oxide in mid-latitudes. Science 283:55-57.
- Stutz J, Ackermann R, Fast JC, Barrie L (2002) Atmospheric reactive chlorine and bromine at the Great Salt Lake, Utah, Geophys Res Lett 29:1380.
- 70. Sullivan RC, et al. (2007) Mineral dust is a sink for chlorine in the marine boundary layer. Atmos Environ 41:7166-7179.
- Thornton BF, et al. (2007) Chlorine activation near the midlatitude tropopause. J Geophys Res 112:D18306.
- 72. Barney WS, et al. (2001) Infrared absorption cross-section measurements for nitrous acid (HONO) at room temperature. J Phys Chem A 105:4166 ibid (2000) 104:1692.

- 73. PNNL Northwest-Infrared Vapor Phase Infrared Spectral Library, Available at URL https://secure2.pnl.gov/nsd/nsd.nsf/Welcome?OpenForm.
- 74. Rivera-Figueroa AM, Sumner AL, Finlayson-Pitts BJ (2003) Laboratory studies of potential mechanisms of renoxification of tropospheric nitric acid. Environ Sci Technol 37:548-554.
- 75. Schmidt MW, et al. (1993) General atomic and molecular electronic structure system. J Comput Chem 14:1347-1363.
- 76. Aikens CM, et al. (2003) A derivation of the frozen-orbital unrestricted open-shell and restricted closed-shell second-order perturbation theory analytic gradient expressions. Theor Chem Acc 110:233-253.
- 77. Frisch MJ, Head-Gordon M, Pople JA (1990) A direct MP2 gradient method. Chem Phys Lett 166:275-280.
- 78. Pople JA, Binkley JS, Seeger R (1976) Theoretical models incorporating electron correlation. Int J Quantum Chem 10:1-19.
- 79. Dunning TH, Jr. (1989) Gaussian basis sets for use in correlated molecular calculations. I. The atoms boron through neon and hydrogen. J Chem Phys 90:1007-1023.
- 80. Woon DE, Dunning TH, Jr. (1993) Gaussian basis sets for use in correlated molecular calculations. III. The atoms aluminum through argon. J Chem Phys 98:1358–1371.
- 81. Baker J (1986) An algorithm for the location of transition states. J Comp Chem
- 82. Culot P, Dive G, Nguyen VH, Ghuysen JM (1992) A quasi-Newton algorithm for first-order saddle-point location. Theor Chim Acta 82:189-205.
- $83. \ \ Helgaker\,T\,(1991)\,Transition-state\,optimizations\,by\,trust-region\,image\,minimization.$ Chem Phys Lett 182:503-510.
- 84. Fletcher GD, Schmidt MW, Gordon MS (1999) Developments in parallel electronic structure theory. Adv Chem Phys 110:267-294.
- 85. Gwinn WD (1971) Normal coordinates, General theory, redundant coordinates, and general analysis using electronic computers. J Chem Phys 55:477-481.
- 86. Baldridge KK, Gordon MS, Steckler R, Truhlar DG (1989) Ab initio reaction paths and direct dynamics calculations. J Phys Chem 93:5107-5119.
- 87. Garrett BC, et al. (1988) Algorithms and accuracy requirements for computing reaction paths by the method of steepest descent. J Phys Chem 92:1476-1488.
- 88. Gonzalez C, Schlegel HB (1989) An improved algorithm for reaction path following. J Chem Phys 90:2154-2161.
- 89. Ishida K, Morokuma K, Komornicki A (1977) The intrinsic reaction coordinate. An ab initio calculation for HNC \rightarrow HCN and H⁻ + CH₄ \rightarrow CH₄ + H. J Chem Phys 66:2153–2156.
- 90. Schmidt MW, Gordon MS, Dupuis M (1985) The intrinsic reaction coordinate and the rotational barrier in silaethylene. J Am Chem Soc 107:2585-2589.
- 91. Gordon MS, Chaban G, Taketsugu T (1996) Interfacing electronic structure theory with dynamics. J Phys Chem 100:11512-11525.
- 92. Taketsugu T, Gordon MS (1995) Dynamic reaction coordinate analysis: An application to $SiH_4 + H^- \rightarrow SiH_5^-$. J Phys Chem 99:8462–8471.
- 93. Maluendes SA, Dupuis M (1990) A dynamic reaction coordinate approach to ab initio reaction pathways: Application to the 1,5-hexadiene Cope rearrangement. J Chem Phys 93:5902-5911.
- 94. Stewart JJP, Davis LP, Burggraf LW (1987) Semi-empirical calculations of molecular trajectories: Method and applications to some simple molecular systems. J Comp
- 95. Takata T, Taketsugu T, Hirao K, Gordon MS (1998) Ab initio potential energy surface by modified Shepard interpolation: Application to the $CH_3 + H_2 \rightarrow CH_4 + H$ reaction. J Chem Phys 109:4281-4289.
- 96. Piecuch P, Kucharski SA, Kowalski K, Musial M (2002) Efficient computer implementation of the renormalized coupled-cluster methods: The R-CCSD[T], R-CCSD(T), CR-CCSD[T], and CR-CCSD(T) approaches. Comp Phys Commun 149:71-96.
- 97. Raghavachari K, Trucks GW, Pople JA, Head-Gordon M (1989) A fifth-order perturbation comparison of electron correlation theories. Chem Phys Lett 157:479–483.
- 98. Russell DJI (2005) NIST Computational Chemistry Comparison and Benchmark Database, NIST Standard Reference Database Number 101 (National Institute of Standards and Technology, Gaithersburg, MD).
- 99. Bode BM, Gordon MS (1998) MacMolPlt: A graphical user interface for GAMESS. J Mol Graphics Model 16:133-138:164.
- 100. Griffin RJ, Dabdub D, Seinfeld JH (2002) Secondary organic aerosol 1. Atmospheric chemical mechanism for production of molecular constituents. J Geophys Res
- 101. Meng Z, Dabdub D, Seinfeld JH (1998) Size-resolved and chemically resolved model or aerosol dynamics. J Geophys Res 103:3419-3435.
- 102. Lewis ER, Schwartz SE (2004) Sea Salt Aerosol Production: Mechanisms, Methods, Measurements and Models—a critical review (American Geophysical Union, Wash-
- 103. Keene WC, et al. (2007) Inorganic chlorine and bromine in coastal New England air during summer. J Geophys Res 112:D10S12.
- 104. Sander SP, et al. (2006) Chemical Kinetics and Photochemical Data for Use in Atmospheric Studies, Evaluation Number 15, JPL Publication 06-2 (Jet Propulsion Laboratory, Pasadena, CA).
- 105. Roehl CM, Orlando JJ, Calvert JG (1992) The temperature dependence of the UVvisible absorption cross-sections of NOCL, J Photochem Photobiol A: Chem 69:1-5.
- 106. Madronich S, Flocke S (1999) in Handbook of Environmental Chemistry, ed Boule P (Springer, Heidelberg).

Corrections

STATISTICS

Correction for "Sequential Monte Carlo without likelihoods," by S. A. Sisson, Y. Fan, and Mark M. Tanaka, which appeared in issue 6, February 6, 2007, of Proc Natl Acad Sci USA (104:1760-1765; first published January 30, 2007; 10.1073/ pnas.0607208104).

The authors note the following: It has been brought to our attention that the algorithm introduced in our paper (ABC-PRC) can produce a biased posterior sample, most noticeably through underestimation in distributional tails. This result occurs as the likelihood ratio in the sequential Monte Carlo incremental weights is approximated by using two unbiased Monte Carlo estimates. One way to avoid a biased posterior sample in the ABC-PRC algorithm is to directly evaluate the importance sampling distribution using a near-optimal backwards kernel. Hence the need for the Monte Carlo estimate in the denominator of the likelihood ratio is circumvented, and an unbiased sampler is obtained. As such, a corrected ABC-PRC algorithm would be:

ABC-PRC Algorithm (corrected):

PRC1 Initialize $\epsilon_1, \dots, \epsilon_T$, and specify initial sampling distribution μ_1 .

Set population indicator t = 1.

PRC2 Set particle indicator i = 1.

PRC2.1 If t = 1 sample $\theta^{**} \sim \mu_1(\theta)$ independently from μ_1 .

If t > 1 sample θ^* from the previous population $\{\theta_{t-1}^{(i)}\}$ with weights $\{W_{t-1}^{(i)}\}$, and perturb the particle to $\theta^{**} \sim K_t(\theta \mid \theta^*)$ according to a transition kernel K_t .

Generate a data set $x^{**} \sim f(x \mid \theta^{**})$. If $\rho(S(x^{**}), S(x_0)) \ge \epsilon_t$ then go to PRC2.1.

PRC2.2 Set

$$\boldsymbol{\theta}_{t}^{(i)} = \boldsymbol{\theta}^{**} \qquad \text{and} \qquad \boldsymbol{W}_{t}^{(i)} = \begin{cases} \pi\left(\boldsymbol{\theta}_{t}^{(i)}\right) \big/ \mu_{1}\left(\boldsymbol{\theta}_{t}^{(i)}\right) & \text{if} \quad t = 1\\ \pi\left(\boldsymbol{\theta}_{t}^{(i)}\right) \big/ \sum_{j=1}^{N} W_{t-1}\left(\boldsymbol{\theta}_{t-1}^{(j)}\right) K_{t}\left(\boldsymbol{\theta}_{t}^{(i)} | \boldsymbol{\theta}_{t-1}^{(j)}\right) & \text{if} \quad t > 1 \end{cases}$$

where $\pi(\theta)$ denotes the prior distribution for θ . If i < N, increment $i = \hat{i} + 1$ and go to PRC2.1.

PRC3 Normalize the weights so that $\sum_{i=1}^{N} W_t^{(i)} = 1$. If $ESS = \left[\sum_{i=1}^{N} (W_t^{(i)})^2\right]^{-1} < E$ then resample with replacement, the particles $\{\theta_t^{(i)}\}$ with weights $\{W_t^{(i)}\}$ to obtain a new population $\{\theta_t^{(i)}\}\$, and set weights $\{W_t^{(i)} = 1/N\}$. PRC4 If t < T, increment t = t + 1 and go to PRC2.

ACKNOWLEDGMENT. The authors thank C. Robert and G. W. Peters for constructive discussion.

www.pnas.org/cgi/doi/10.1073/pnas.0908847106

COMMENTARY

Correction for "A curvy, stretchy future for electronics," by John A. Rogers and Yonggang Huang, which appeared in issue 27, July 7, 2009, of Proc Natl Acad Sci USA (106:10875-10876; first published June 30, 2009; 10.1073/pnas.0905723106).

The authors note that on page 10875, right column, the sentence beginning on line 22, "For example, ultrathin sheets of silicon are flexible, for the same reason that any material in thin film form is flexible: bending strains are inversely proportional to thickness" should instead appear as "For example, ultrathin sheets of silicon are flexible, for the same reason that any material in thin film form is flexible: bending strains are directly proportional to thickness."

www.pnas.org/cgi/doi/10.1073/pnas.0908993106

ENVIRONMENTAL SCIENCES, CHEMISTRY

Correction for "Chlorine activation indoors and outdoors via surface-mediated reactions of nitrogen oxides with hydrogen chloride," by Jonathan D. Raff, Bosiljka Njegic, Wayne L. Chang, Mark S. Gordon, Donald Dabdub, R. Benny Gerber, and Barbara J. Finlayson-Pitts, which appeared in issue 33, August 18, 2009, of *Proc Natl Acad Sci USA* (106:13647–13654; first published July 20, 2009; 10.1073/pnas.0904195106).

The authors note that on page 13648, Equation 5 appeared incorrectly. Further, in Equation 6 on page 13649, the formula for nitryl chloride should have read: ClNO₂. These errors do not affect the conclusions of the article. The corrected equations appear below.

$$NO^+NO_3^- + HCl \rightarrow CINO + HNO_3$$
 [5]

$$NO_2^+NO_3^- + HCl \rightarrow ClNO_2 + HNO_3$$
 [6]

www.pnas.org/cgi/doi/10.1073/pnas.0909721106